



**HAL**  
open science

# Chaotic motion of charged particles in toroidal magnetic configurations

Benjamin Cambon, Xavier Leoncini, Michel Vittot, Rémi Dumont, Xavier Garbet

► **To cite this version:**

Benjamin Cambon, Xavier Leoncini, Michel Vittot, Rémi Dumont, Xavier Garbet. Chaotic motion of charged particles in toroidal magnetic configurations. 2014. hal-00945145v1

**HAL Id: hal-00945145**

**<https://hal.science/hal-00945145v1>**

Preprint submitted on 11 Feb 2014 (v1), last revised 4 Dec 2014 (v2)

**HAL** is a multi-disciplinary open access archive for the deposit and dissemination of scientific research documents, whether they are published or not. The documents may come from teaching and research institutions in France or abroad, or from public or private research centers.

L'archive ouverte pluridisciplinaire **HAL**, est destinée au dépôt et à la diffusion de documents scientifiques de niveau recherche, publiés ou non, émanant des établissements d'enseignement et de recherche français ou étrangers, des laboratoires publics ou privés.

# Chaotic motion of charged particles in toroidal magnetic configurations

Benjamin Cambon, Xavier Leoncini, Michel Vittot  
*Aix Marseille Université, CNRS, CPT, UMR 7332, 13288 Marseille, France and  
Université de Toulon, CNRS, CPT, UMR 7332, 83957 La Garde, France*

Rémi Dumont, Xavier Garbet  
*Institut de Recherche sur la Fusion par confinement Magnétique, CEA Cadarache F-13108 St-Paul-Lez-Durance*

We study the motion of a charged particle in a tokamak magnetic field and discuss its chaotic nature. Contrary to most of recent studies, we do not make any assumption on any constant of the motion and solve numerically the cyclotron gyration using Hamiltonian formalism. We take advantage of a symplectic integrator allowing us to make long-time simulations. First considering an idealized magnetic configuration, we add a non generic perturbation corresponding to a magnetic ripple, breaking one of the invariant of the motion. Chaotic motion is then observed and opens questions about the link between chaos of magnetic field lines and chaos of particle trajectories. Second, we return to a axi-symmetric configuration and tune the safety factor (magnetic configuration) in order to recover chaotic motion. In this last setting with two constants of the motion, the presence of chaos implies that no third global constant exists, we highlight this fact by looking at variations of the first order of the magnetic moment in this chaotic setting. We are facing a mixed phase space with both regular and chaotic regions and point out the difficulties in performing a global reduction such as gyrokinetics.

## I. INTRODUCTION

The motion of charged particles in a magnetic field is a classical issue of dynamical systems and plasma physics, as for instance the the fifty years old study made in [1, 2], before a time when numerical simulations became mainstream, or more recent approaches as for instance [3, 4]. Usually, main properties of particle trajectories strongly depend on the form of magnetic field lines, making global features difficult to determine without using basic approximations. That's why, the theory of plasma confinement into a tokamak magnetic field is often studied using gyrokinetic theory. One of the assumptions made by regular codes based on this approach is that the magnetic moment  $\mu$  of confined particles is constant[5–7]. The straight consequence is to consider that particle trajectories are integrable for axi-symmetric configuration and no electric field.

Indeed, trajectory of a charged particle in a tokamak idealized magnetic field is a six dimensions system in which we can consider two exact invariants, the energy and the angular momentum related to the toroidal invariance of the field. Moreover, the magnetic moment is said to be an adiabatic invariant. So, in good conditions,  $\mu$  is a quasi-constant on short time but has some variations over very large-time scales (see for instance [8–12]). Due to Arnold-Liouville Theorem, integrability of charged particle trajectory requires three exact commuting invariants [13]. Suppose that this three quantities commute, which is not obvious, we can transform the original system into an integrable approximation. However this may change the nature of particles trajectories. These remarks lay the ground for possible presence of Hamiltonian chaos of particle trajectory and a non-constant magnetic moment even in an idealized magnetic case.

In this paper, we integrate the Hamilton equations

through a symplectic code to be able to solve on one part the cyclotron motion on short time, and on an other part, to make long-time simulations, without approximations. Moreover, contrary to classical approach based on Runge-Kutta method, the main advantage of the symplectic codes is to keep constant the invariants of the motion over large-time scales, allowing us to study adiabatic variation of the magnetic moment.

Using this property, the question we would like to answer is the presence of Hamiltonian chaos in charged particle motion in a toroidal magnetic field, studying two different cases. First, we add a non generic magnetic ripple due to the finite number of coils surrounding the tokamak chamber, breaking one of the invariant of the motion. In a second case, we want to create chaos to particle trajectories keeping an idealized magnetic field but looking for chaos in a six-dimensional system is not simple. In order to find the chaotic regions of the phase space, we decide to study the limit case in which the aspect ration (major radius vs minor one) of the tokamak tends to infinity. In this limit, the tokamak becomes a cylinder and the motions of the charged particles are integrable. The method is to create a separatrix in this simple system using the fact that the poloidal part of the magnetic field in the tokamak chamber is not a well-known function. Then, we will return to the toroidal case and look at the alteration of the integrability of the particle trajectories around the separatrix. In the same time, this second method highlights variations of the magnetic moment.

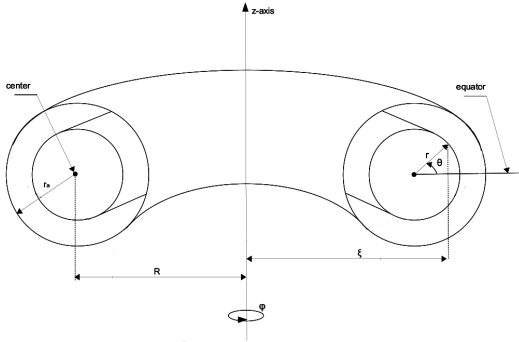


Figure 1: Toroidal geometry and notations

## II. MODEL

### A. Basic equations

A schematic view of the toroidal geometry is presented on fig 1. In the  $(r, \theta, \varphi)$  coordinates, we shall first consider the tokamak magnetic field of the following form [14]:

$$\mathbf{B} = \frac{B_0 R}{\xi} (\hat{\mathbf{e}}_\varphi + f(r) \hat{\mathbf{e}}_\theta), \quad (1)$$

in which  $\xi = R + r \cos(\theta)$ ,  $\hat{\mathbf{e}}_\varphi$  and  $\hat{\mathbf{e}}_\theta$  are the unit vectors associated respectively to the  $\varphi$  and  $\theta$  directions. The toroidal component along  $\hat{\mathbf{e}}_\varphi$  of the magnetic field is due to external coils around the tokamak chamber whereas the plasma generated current inside the tokamak leads to the creation of the poloidal component  $\hat{\mathbf{e}}_\theta$ . In this approximation the function  $f(r)$  represents the amplitude of the poloidal field as a function of the radius and it is directly connected to the so-called safety factor  $Q$  of principal importance in tokamak physics :

$$f = r/Q\xi \approx r/QR. \quad (2)$$

In Eq. (2) for simplicity we shall use the approximation in order to simply have  $Q = Q(r)$ . Usually, the amplitude of the poloidal component is estimated at about 10% of the global magnetic field but the safety factor is not an a priori fixed function and can actually be tuned in some machines. So, respecting the flux conservation of the magnetic field  $\nabla \cdot \mathbf{B} = 0$ , we have the freedom to choose the function  $f(r)$ . It is easy to show that any smooth function depending only on  $r$  satisfies the flux conservation constraint.

Associated to Eq. (1), a vector potential can be chosen respecting the Coulomb gauge :

$$\mathbf{A}(r) = B_0 \frac{F(r)}{\xi} \hat{\mathbf{e}}_\varphi - B_0 R \log\left(\frac{\xi}{R}\right) \hat{\mathbf{e}}_z, \quad (3)$$

where  $F(r) = \int^r f$ . This choice of the magnetic field and associated potential vector corresponds nested circular magnetic surfaces, which is a good approximation in the large aspect ratio limit. In a more realistic situation, we may have for instance to take into account that the magnetic surfaces have a slowly drifting center.

Given the magnetic field we consider the dynamics of a particle with charge  $e$  and mass  $m$ , in this magnetic field. The Hamiltonian of the system writes

$$H = \frac{(\mathbf{p} - e\mathbf{A})^2}{2m}, \quad (4)$$

where  $\mathbf{p} = (p_x, p_y, p_z)$  and  $\mathbf{q} = (x, y, z)$  form three pairs of canonically conjugate variables. The associated equations of motion are :

$$\begin{cases} \dot{\mathbf{q}} = (\mathbf{p} - e\mathbf{A})/m, \\ \dot{\mathbf{p}} = \frac{e}{m} (\nabla \mathbf{A}) \cdot (\mathbf{p} - e\mathbf{A}). \end{cases} \quad (5)$$

The second equation can be more explicitly written as

$$\dot{p}_i = \frac{e}{m} \left[ (p_x - eA_x) \frac{\partial A_x}{\partial i} + (p_y - eA_y) \frac{\partial A_y}{\partial i} + (p_z - eA_z) \frac{\partial A_z}{\partial i} \right], \quad (6)$$

in which  $i$  represents  $x, y$  or  $z$ . We readily notice in (5) that the particle velocity  $\dot{\mathbf{q}}$  is given by  $\mathbf{v} = (\mathbf{p} - e\mathbf{A})/m$ .

### B. Chaos, invariants and Adiabatic approximation

Looking for chaotic aspects of particle motions leads to look at the invariants of this three-dimensional system. Indeed, finding three independent invariants commuting with each other would imply integrability in the sense of Arnold-Liouville [13]. The energy of the particle is an exact invariant equal to  $H = \frac{1}{2}m\mathbf{v}^2$ . Then in the case of the magnetic field (1), the system is invariant by rotation around the  $\hat{\mathbf{e}}_\varphi$  axis. This entails that the conjugated angular momentum  $M$  is a constant of the motion (Noether Theorem). We can define it using the Lagrangian

$$\mathcal{L} = \frac{1}{2}m\mathbf{v}^2 + e\mathbf{A} \cdot \mathbf{v}, \quad (7)$$

by

$$M = \frac{\partial \mathcal{L}}{\partial \frac{d\varphi}{dt}}. \quad (8)$$

Using this definition (8) and the value of the vector potential in the proposed gauge, we obtain

$$M = \zeta \mathbf{p} \cdot \hat{\mathbf{e}}_\varphi. \quad (9)$$

Besides these two exact constants of the motion, we need a third integral in order to get integrable motion. The

third constant that is that is often used is the magnetic moment  $\mu$  defined at leading order by :

$$\mu = \frac{m\mathbf{v}_\perp^2}{2B}, \quad (10)$$

where  $\mathbf{v}_\perp$  denotes the component of the velocity  $\mathbf{v}$  perpendicular to the magnetic field  $\mathbf{B}$ . The magnetic moment (10) of a gyrating particle is used as a constant even though it is often only an adiabatic invariant [15–18]. Assuming that these three integrals are in involution we end up with an integrable system. Besides the involution, it is not obvious that the adiabatic invariant is actually a real invariant, in fact it is likely that depending on the magnetic configuration, this assumption breaks down in some regions of phase space, leading to local Hamiltonian chaos. The breaking of this assumption could be problematic, especially since in the last fifteen years a considerable effort had been devoted to gyrokinetics. Hot magnetized plasmas are usually well described using a Maxwell-Vlasov or Vlasov-Poisson description. This implies working with a time dependent particle density function in six-dimensions. In gyrokinetics theory the adiabatic invariant is used to reduce the dimensionality of phase space. This allows to not only to move to an effective  $4 + 1$  dimensional phase space, but allows also to avoid resolving in time the fast gyration around field lines (cyclotron frequency), both of these features are very appealing when aspiring at a full fledged numerical simulation of magnetized fusion plasmas in realistic conditions. In this paper we do not consider the consequences of the presence of Hamiltonian chaos on this theory, we however will look for the breaking of the adiabatic invariant. In this spirit we consider so-called fast-particles, meaning in typical tokamak conditions, we consider particles whose energy is from  $10keV$  to around  $3.5MeV$ , which is about the energy of  $\alpha$ -particles resulting from the fusion of Deuterium and Tritium nuclei. Looking at the variation of  $\mu$  given by Eq. (10) on times shorter than the cyclotron period, we observe a non constant function, which at first approximation looks like a sinusoid with a specific period. Given this fact, in what follows we now consider the average of  $\mu$  on one or more cyclotron period as the effective adiabatic invariant, but keep the same notation.

In order to look for chaos, a possibility would be to actually find traces of adiabatic chaos, meaning chaos on adiabatic time scales. So, looking for main characteristic of the motion of the particle, we have to study long-term variations of  $\mu$ . The requirements for a numerical approach are thus that we must resolve short time variation meaning the fast cyclotron motion but we also have to simulate on very long time to be able to capture possible fluctuations of the magnetic moment. We therefore need to use a symplectic approach.

### C. Numerical scheme

It is well known that using a classical Runge-Kutta scheme leads to important long-time errors. Indeed the scheme is usually not symplectic, hence the time steps does not preserve efficiently phase-space volume, in this case long-time studies can lead to the emergence of sinks, sources and attractors, which do not belong to the realm of Hamiltonian chaos see for instance field lines in [19]. In order to avoid this difficulty, numerical simulations have been performed using the sixth order Gauss-Legendre symplectic scheme discussed in [20]. Since we needed pairs of canonically conjugated variables, we remained in Cartesian coordinates. This construction ensures for instance the stability of the constants of the motion even for very large times. Last but not least, in order to minimize numerical errors due truncations we use dimensionless variables. This allows use variables whose variations remain in a finite range. Our choice is performed as follows, noting  $\tilde{r}$ ,  $\tilde{t}$  and  $\tilde{B}$  our new variables. We write :

$$\tilde{r} = r/r_a, \quad (11)$$

$$\tilde{t} = \omega_c t = \frac{m}{eB_0} t, \quad (12)$$

$$\tilde{B} = B/B_0, \quad (13)$$

where  $r_a$  is the minor radius (see Fig. 1),  $\omega_c$  is the cyclotron frequency, and  $B_0$  is the typical magnetic intensity at the center of the torus. Thereafter, we will only consider these dimensionless variables, and for clarity and readability we drop the  $\tilde{}$  and note  $(r, t, B)$  the dimensionless variables.

In order to validate the accuracy of our numerical scheme and test our code, we first consider the particular case for which there is no plasma inside the tokamak. In this configuration, the poloidal magnetic field is negligible. This property entails that the magnetic field depends only on  $\xi$ . So, in polar coordinates  $(\xi, \varphi, z)$ ,  $\mathbf{B} = R\hat{e}_\varphi/r_a\xi$ . The application of Newton's second law, which computation is detailed in annex V A, demonstrates the drift of the particle in  $z$ -direction (the direction depends on the sign of the charge). In fact the system resumes to an integrable one and we end up with an effective Hamiltonian :

$$H_{eff_0} = \frac{\xi^2}{2} + \frac{C^2}{2\xi^2} + \frac{\ln^2(\xi)}{4} + C'\ln(\xi), \quad (14)$$

in which  $C = \xi^2\dot{\varphi}$  and  $C'$  are constants, which depend on the particle's initial conditions. A comparison between the  $(\xi, \dot{\xi})$  phase portrait obtained by our numerical scheme and the one obtained by resolving the quadrature, using the Hamiltonian (14) is shown in Fig. 2. We can notice an excellent agreement between the two curves, which validates our code. To be more specific, the step time is chosen to be  $\delta t = 0.01$ , which means we should

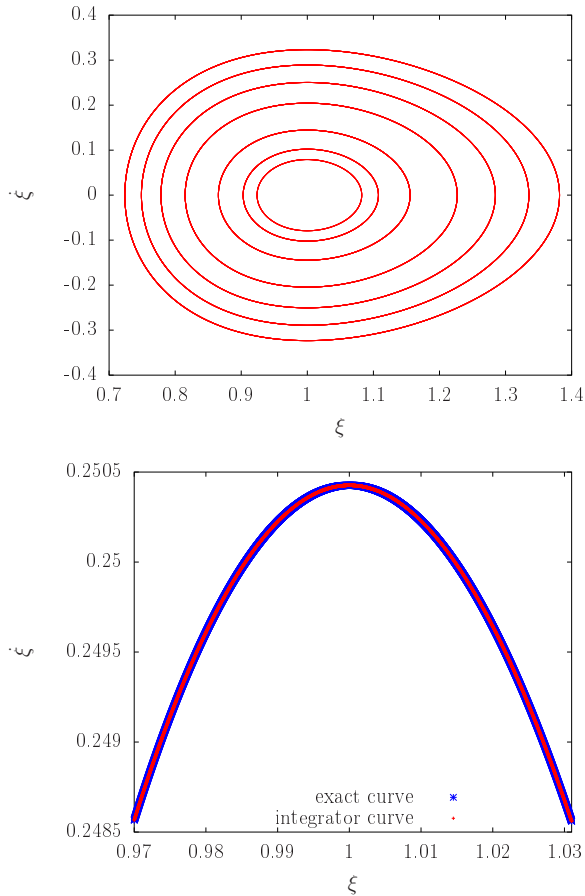


Figure 2: Top: phase portrait in  $(\xi, \dot{\xi})$  coordinates for the simple case without plasma in the tokamak chamber. Bottom: zoom and comparison between a numerically computed trajectory and the analytical one. Numerical integration is performed for  $4 \cdot 10^7$  time steps using a  $\delta t = 0.01$ .

have about 100 points to resolve the gyration motion. The records in Fig. 2 cover a period of  $4 \cdot 10^7$  time steps with  $R = 3$ ,  $C = 1$  and  $C' = 0$ . Further analysis of the Hamiltonian (14), leads as conclusions that there are no separatrix in phase space and that the equilibrium point corresponds to a linear drift of the particle while all other trajectories are helical. As can be noted in Fig. 2, when we zoom on one curve, we can compare in blue the exact trajectory and in red the motion computed by the integrator. The two methods give the same results with a precision better than our recorded digits, meaning better than  $10^{-5}$ . Another check of the numerical accuracy of our computation will be performed in Sect. IV.

### III. CHAOTIC TRAJECTORIES USING RIPPLE EFFECT

#### A. The plasma with cylindrical symmetry first part

In the more general case when a plasma is present in the tokamak, the  $(\xi, \dot{\xi})$  plane loses its specificity because the magnetic field  $\mathbf{B}$  also depends on  $r$  through the expression of the safety factor. In order to choose a configuration (15), we take a function that satisfies  $Q(0) = 1$ , that presents a maxima and that respects  $\lim_{r \rightarrow \infty} Q(r) = 0$  :

$$Q(r) = \frac{1 + ar}{1 + r^2}, \quad (15)$$

we recover the magnetic profile and the function  $f(r)$  using the approximate expression in (2). In the following, we will fix the constant  $a = 10$ . It becomes then challenging to visualize trajectories in the sixth-dimensional phase space. Indeed, the existence of two exact first integrals leaves room for possible chaos, moreover the expected cyclotronic motion of charged particles is likely to blur sections. Choosing a good section for visualizing trajectories becomes therefore challenging. The first problem is related to the choice of the initial conditions in a six-dimensional phase space. If we focus on fast particles corresponding to the ashes of fusion, their initial conditions are not explicitly known, however we can consider that their energy (mostly a kinetic one) is more or less known and about 3.5MeV and that their initial location is close to the center of the chamber, where the plasma is dense and hot and fusion reactions take place. However, the direction of the speed is uncertain, leaving us with two independent parameters, the norm being fixed by a chosen energy. Then we have to find a suitable section in which we can distinguish integrable and chaotic trajectories. If we only consider a classical section is the poloidal  $(\xi, z)$  plane with a fixed angle, things are not clear due to the Larmor gyration, we end up with thick trajectories for all types of initial conditions. In order to better visualize we have considered to possible options. In a first attempt we computed the time average of  $\mu(t)$  over a large number gyrations

$$\bar{\mu}(\tau) = \frac{1}{\tau} \int_0^\tau \mu(t') dt'. \quad (16)$$

Typically we computed  $\bar{\mu}$  during a given initial time of the trajectory. We then performed a section  $(\xi, z)$  and recorded positions each time  $\mu(t) = \bar{\mu}$  and  $d\mu/dt > 0$ . We then get clear thin and distinct integrable trajectory. However for extreme initial conditions, we noticed a slow drift in  $\mu(\tau)$  such that we could not record any data after a while as  $\mu(t)$  was not crossing the initially computed  $\bar{\mu}$  value. In order to circumvent this last problem and noticing that  $\mu(t)$  always had a fast oscillating component, we finally settled for the following section: we only

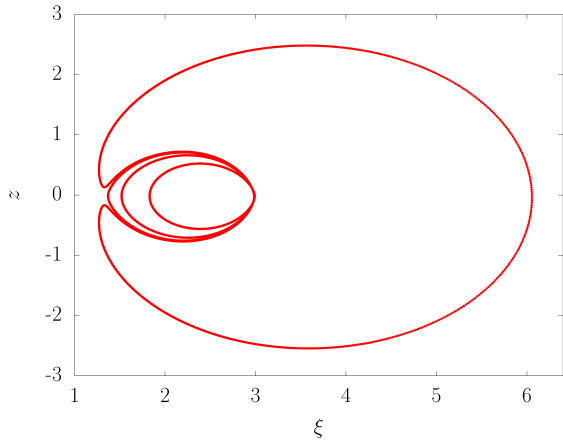


Figure 3:  $(\xi, z)$  section obtained with  $d\mu/dt = 0$  with no ripple. Four different trajectories with different energies but same speed directions are displayed. Motion appears as integrable, we notice the presence of a separatrix, distinguishing to types of orbits: so called passing orbits and banana orbits.

record points when reaching local maxima of  $\mu(t)$ , meaning we plot the points when  $d\mu/dt = 0$  and  $d^2\mu/dt^2 < 0$ . As a consequence, plotted points correspond to one Larmor gyration. The resulting  $(\xi, z)$  section is presented in Fig. 3, where different trajectories are represented and have different values of the energy but the same initial speed direction. On this this section, we see two different kinds of trajectories: the elliptic ones (corresponding to so-called passing particles) and the bananas, separated by a separatrix. They all appear to be integrable, and looking for Hamiltonian chaos is not easy. Indeed in this setting, because the localization of the separatrix appears to depend on the initial speed direction, so on one section we can only represent particles with the same speed directions and location initial conditions, else we actually end up with a projection and crossing trajectories. In order to look for Hamiltonian chaos one of the solutions is to add a perturbation into the magnetic field.

### B. The ripple effect

In order to trigger chaos more efficiently, we have introduced so called-ripple effect [21]. This effect is mainly due to the finite number of coils around the tokamak and leads to the breaking of the toroidal invariance of the magnetic field, with for instance the dependance of the magnetic field on toroidal angle  $\varphi$ . A direct consequence of the symmetry breaking is that the angular momentum  $M$  ceases to be an invariant, the accessible phase space becomes larger and chaos can occur even if another “hidden” constant of the motion related to the magnetic moment exists.

In order to remain simple we shall consider a very specific and actually non generic perturbation. This trans-

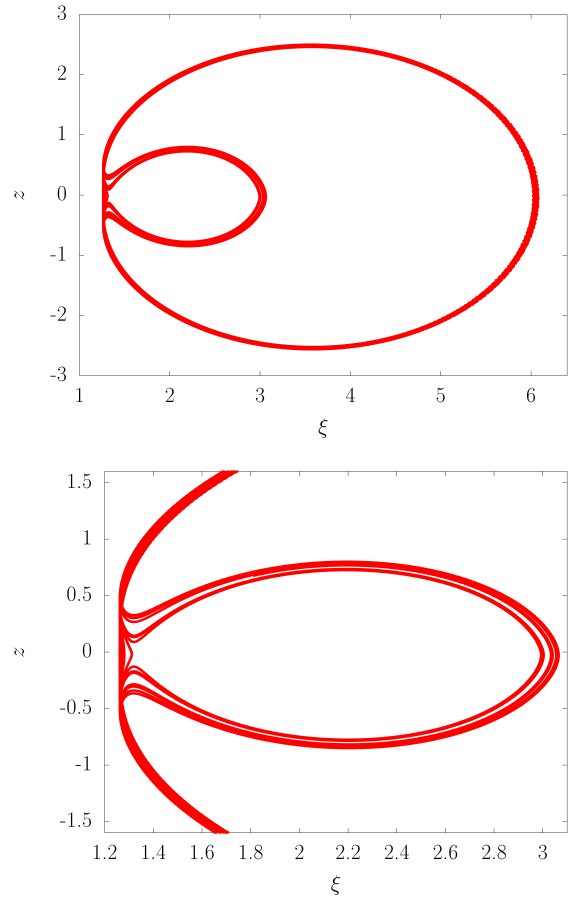


Figure 4: Top:  $(\xi, z)$  section obtained with  $d\mu/dt = 0$ , and one trajectory with ripple and  $\varepsilon = 0.2$ . Bottom: zoom of the section near the separatrix, we see the jumps between the passing orbits and the banana one.

late into a vector potential modified as:

$$\mathbf{A}(r) = \frac{F(r)}{\xi}(1 + \delta \cos(k\varphi))\hat{\mathbf{e}}_\varphi - \log(\xi)\hat{\mathbf{e}}_z, \quad (17)$$

in which  $\delta$  represents the amplitude of the perturbation entailed by the ripple and  $k$  the number of coils. In the case of ITER,  $k = 18$  and  $\delta$  is estimated to  $10^{-3}$  (the expression is of the perturbation is though different). As mentioned the breaking of one of the exact invariant of the motion makes easier the search of chaotic motion because the trajectory is now confined in a five dimensional phase space. We show in Fig. 4 the motion of one charged particle in the perturbed magnetic field, but for a perturbation amplitude  $\delta = 0.2$ . Contrary to the idealized magnetic case, chaos shows up and is characterized by separatrix breaking. Starting from a banana motion, the particle trajectory is able to cross the separatrix to become an elliptic passing one and vice versa. We though would like to insist that a priori we remain in a situation with mixed phase space. In the sense that if we start at a sufficiently low energy, far from the separatrix with

an elliptic trajectory, the motion does not present sign of chaos at least for the length of time during which we computed and observed such trajectories.

### C. Link between chaos of magnetic field lines and chaotic trajectories of charged particles

One of the usual cartoons that is used when describing magnetic confinement, is that particles have a fast gyration around magnetic field lines, and if the Larmor radius is small, particles follow more or less field lines. When looking at the previous sections in Fig. 3, we directly see that this is likely not the case. However this remark, lead to numerous studies on the chaoticity of magnetic field lines, having in mind a picture very much like the advection of passive tracers in a stationary three dimensional flows, where passive tracers simply follows velocity field lines [19, 22–31]. The tokamak being a three dimensional object, it has been shown for a long time that field lines of flux conservative fields are generically chaotic in three dimensions. Assuming particles follow field lines it becomes natural to infer that studying the chaos of field lines would have a direct impact on particles confinement and trajectories. In the ideal tokamak like magnetic fields, the magnetic field lines are not chaotic, due to the existence of the existence of the invariance by rotation of an angle  $\varphi$ . In the chosen magnetic fields, the lines winds helically around a given torus. Breaking the invariance, would lead to a real three dimensional system and chaos of lines. It is in this sense that the perturbation chosen in Eq. (17) is non generic. Indeed in this last expression the magnetic field still does not depend on  $r$ , nor has a component along  $\hat{r}$ , hence the magnetic field lines still gently wind around a torus, the variation of intensity is compensated by a non uniform winding, which allows to keep a constant flux across a given disk of radius  $r$ . Field lines are therefore still integrable, and a Poincaré section of these lines would not differ from the perfectly invariant case.

We insist therefore on the fact that despite the regularity of field lines, we end up with chaotic particle trajectories. The connection between the two being therefore not obvious. Given this remark, we shall reconsider the case with an rotational invariance, and see if we can also find chaotic motion of charged particle. In order to illustrated this we reconsider our point of view and start with a cylindrical plasma tube instead of an empty toroidal solenoid.

## IV. IMPACT OF THE TOROIDAL GEOMETRY INTO PARTICLE TRAJECTORIES

### A. Infinite torus

In this section, we will use an other approach to create chaotic trajectories in a tokamak magnetic field. For

this purpose we first consider the case of a cylindrical magnetic geometry, which is the limit, when  $R$  tends to infinity, of the toroidal system. In this approximation,  $\hat{e}_\varphi$  becomes a stationary vector and the idealized magnetic field can be rewritten as:

$$\mathbf{B} = B_0(\hat{e}_\varphi + f(r)\hat{e}_\theta). \quad (18)$$

A calculation described in appendix VB leads to an integrable system with a new effective Hamiltonian:

$$H_{eff} = \frac{\dot{r}^2}{2} + \frac{C''^2}{2r^2} + \frac{r^2}{8} + \frac{F^2(r)}{2} = E_c + V_0(r) + \frac{F^2(r)}{2}, \quad (19)$$

in which

$$C'' = r(v_\theta + r/2) \quad (20)$$

is a constant. The potential  $V_0(r)$  tends to infinity when  $r$  tends to zero or infinity. Between these limits, it admits a minimum at  $r_0 = \sqrt{2C''}$ . We can thus tune the function  $F(r)$  in order to generate a separatrix in this cylindrical system. For this purpose we create a local maximum for effective potential energy. We remark that choosing a  $F(r)$ , corresponds to fixing a specific so called  $Q$ -profile of the tokamak plasma magnetic confinement. We will then consider perturbation as the deformation and the returning to a toroidal geometry, decreasing the value of  $R$ . A possible choice for  $F$  can be :

$$F = ar^2 \exp\left(-\frac{r^2}{c^2}\right), \quad (21)$$

with  $a = 30$  and  $c = \sqrt{100}$ . The details of the initial conditions which are fixed by  $C''$  and  $H_{eff}$  is explained in appendix VB. Considering these, the figure 5 shows the phase space  $(r, \dot{r})$  of the system for a proton with the particular condition  $C'' = \sqrt{10^{-5}}$ .

As expected, the motion depicted on Fig. 5 shows that the particle trajectory in this type of magnetic field is integrable. We visualize the separatrix between two areas corresponding to the potential wells and the rest of the phase space for particles with an energy of about  $E = 600keV$ . This gives us another framework to successfully test the accuracy of our numerical integration, especially in the vicinity of the separatrix as described in Fig. 5.

Looking for chaos, we shall perturb this system going back to the toroidal geometry and study the impact of the curvature onto trajectory properties.

### B. Particle trajectories in toroidal geometry

As mentioned we consider the toroidal aspect with finite large radius of the tokamak as a perturbation of the cylindrical system. We now consider finite radius  $R$ , and will slowly increase the ‘‘perturbation’’ by decreasing the value of  $R$ . We are eager to compare the motion of a

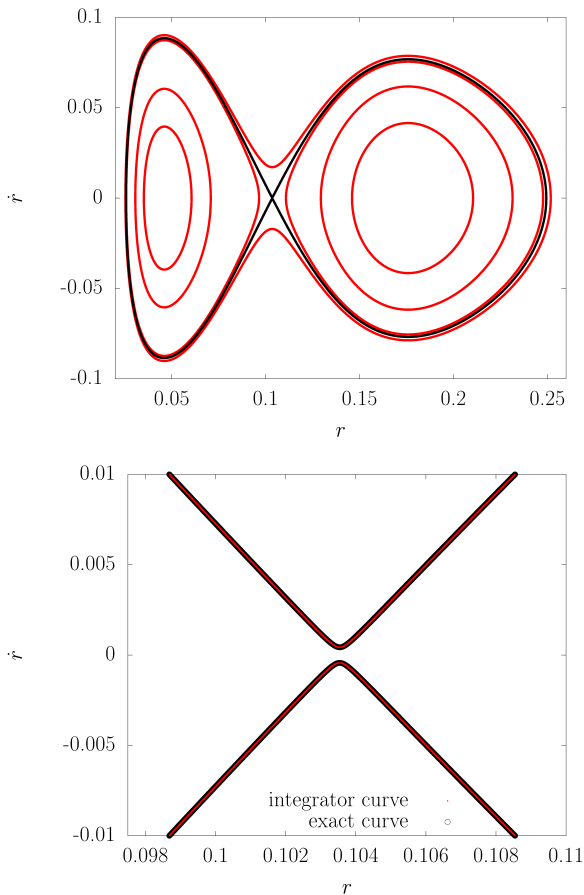


Figure 5: Top: phase space for a particle in the cylindrical magnetic field governed by Hamiltonian (19). Bottom: zoom near the separatrix and comparison between analytical curve solved by quadrature and numerical integration.

charged particle in the cylindrical geometry to the one in the toroidal system. For this purpose we shall visualize the particle trajectories in the  $(r, \dot{r})$  plane. In order to perform a clean section, considering the action-angle variables associated to the integrable Hamiltonian (19), section are usually best performed at constant action. Indeed if we only consider a projection on the  $(r, \dot{r})$  plane, as previously, the Larmor radius causes that we end up with thick trajectories for all trajectories. Since computing the action is not a straightforward task, we shall use the fact that for integrable systems  $H = H(I)$ , a section at constant  $I$ , corresponds to a section at constant energy. For this purpose, we reconsider the effective Hamiltonian  $H_{eff}$  (19), which in the cylindrical case can be rewritten as

$$H_{eff} = \frac{v_r^2}{2} + \frac{C''^2}{2r^2} + \frac{r^2}{8} + \frac{v_\varphi^2}{2}, \quad (22)$$

and given the expression of  $C''$  (20) we notice it corresponds to the actual kinetic energy of the system up to some constant ( $2C''$ ). However for a finite radius this Hamiltonian presents temporal variation and becomes a

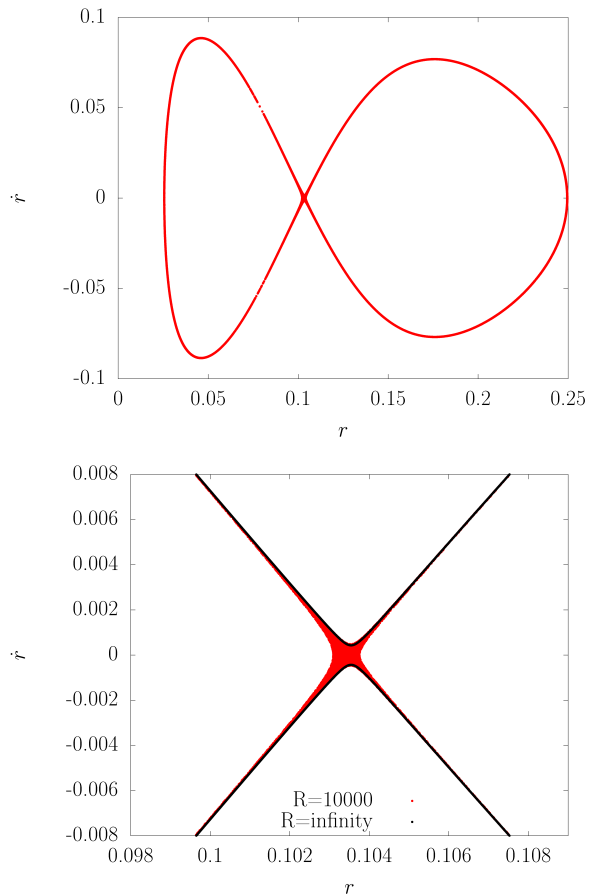


Figure 6: Top:  $(r, \dot{r})$  section for  $H_{eff} = Constant$ ,  $R = 10000$ ,  $E = 600keV$ . Initial conditions are identical to the ones taken in the cylindrical case near the separatrix in Fig. 5. Bottom: zoom of the trajectory near the unstable fix point, the integrable trajectory is drawn for comparison. Hamiltonian separatrix chaos emerges.

time dependent function  $H_{eff}(t)$ . Its expression does not change but, in the toroidal system,  $C''^2$  is not a constant anymore. So performing a section at constant action corresponds to perform a section at constant  $H_{eff}$ , which corresponds to a section taken at constant  $C''$ , since of course the kinetic energy of a particle is a constant of the motion.

We first start with a small perturbation, namely  $R = 10000$  (in our dimensionless units  $R$  is measured in minor radii). Results are displayed in Fig. 6. In fact most of the trajectories remain regular, but when we consider a particle with initial conditions close to separatrix in the integrable cylindrical case, represented in Fig. 6. In fact, the overall picture has the same aspect as the cylindrical phase space (Fig. 5), except if we zoom around the unstable equilibrium point, the dynamics becomes very different and we see the emergence of a chaotic region, often dubbed a stochastic layer. As in Sect. III, the chaotic region is created by the breaking of the separatrix, in the current case we remain however with an axi-symmetric

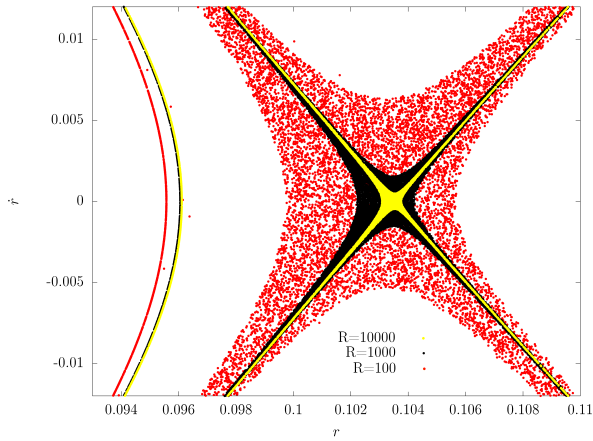


Figure 7:  $(r, \dot{r})$  sections for  $H_{eff} = \text{Constant}$  and  $R = 10000, 1000, 100$ . We see an increase of the stochastic layer as the major radius is reduced. For  $R = 100$ , we start to see some problems with the section (see Fig. 8). For comparison tori corresponding to identical initial conditions and the different radii are drawn in the regular region. Final time is  $t = 610^4$ . For each regular trajectory the initial conditions are:  $x_0 = R + 0.05$ ,  $y = 0$ ,  $z = 0$ ,  $vy = -F(r(t=0))$ ,  $vz = -(C''/(x-R) - (x-R)/2.0)$ ,  $E = 590\text{keV}$ ,  $v = \sqrt{2E/m}$ ,  $vx = \sqrt{v^2 - vy^2 - vz^2}$ , for the chaotic trajectories they are the same but with  $E = 600\text{keV}$ .

case. As such the presence of chaos indicates that the system is non-integrable and de facto rules out the existence of a third constant of the motion, for instance one related to the magnetic moment.

In order to have a clearer picture we increase the perturbation and we decrease progressively  $R$  from  $R = 10000$  to  $R = 100$ . The global picture are displayed in Fig. 7. We consider the same initial condition and display the section of one trajectory, we confirm the expected trend that increasing the perturbation, corresponding to a reduction of the aspect ratio  $R$  leads to a growth of the chaotic region in the phase space. In order to be more conclusive, we as well display regular trajectories obtained in these three settings using the same initial condition as well. The emergence of chaos is a priori not a numerical artifact. When further decreasing  $R$ , we notice that another phenomenon appears when we pass from  $R = 100$  to  $R = 10$ , see the section for  $R = 10$  and  $R = 3$  depicted in Fig. 8 and a global apparent increase of chaos. It is though likely that in this range, the section at constant action is not suitable to correctly describe the system, this is relatively surprising as the perturbation is still relatively small and we are actually reaching the aspect ratio of real machines such as the one of ITER for instance. The problem of creating a good section in this region needs still to be solved, and one of the problems of remaining with section made using the cylindrical action could be related to monodromy issues.

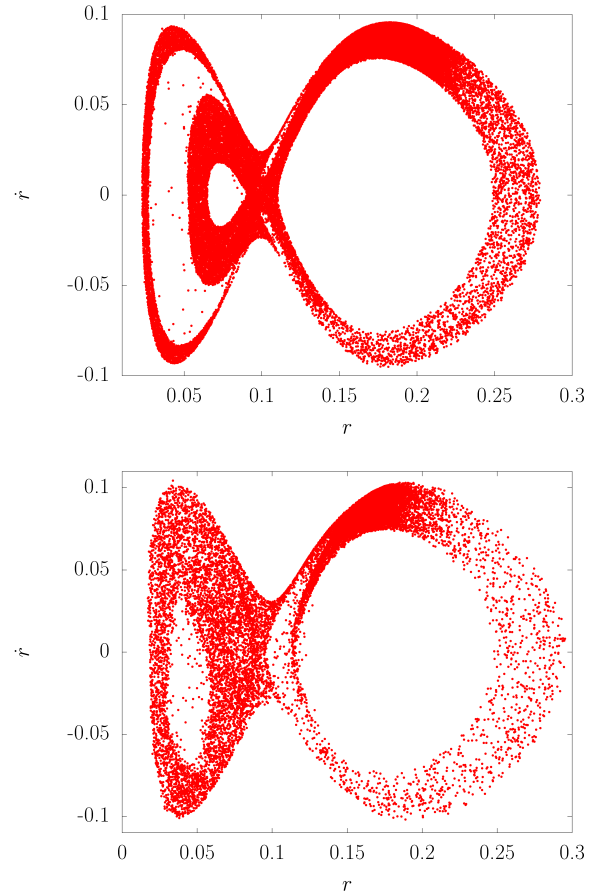


Figure 8: Top:  $(r, \dot{r})$  section for  $H_{eff} = \text{Constant}$ , with  $R = 10$ ,  $E = 600\text{keV}$ . Initial conditions are identical to the previous cases, meaning the one taken in the cylindrical case near the separatrix in Fig. 5. Bottom, same section but with  $R = 3$ . We notice in both plots what looks like an increase of chaos, but that also that the sections at constant action appears as non satisfactory anymore.

### C. Variation of the magnetic moment $\mu$

As previously discussed the presence of chaos in an axially symmetric system with already two constant of the motion, leads to imply to the system is not integrable and as such it would preclude the existence of a third constant of the motion, notably one related to the magnetic momentum. In order to check this statement we measured the variations of the magnetic momentum using time averages of expression (10). For this purpose we compare three different cases in Fig. 9. In this figure, the average  $\bar{\mu}$  are computed on about one hundred cyclotron gyrations. Except for initial kinetic the energy, the three cases have identical initial conditions. In the first case (upper plot), we take  $R = 10000$  and an energy of about  $E = 450\text{keV}$ , this leads to an integrable trajectory, associated to this characteristics, we note that the variations of  $\bar{\mu}$  are small and periodic. In the second case (middle plot of Fig. 9) we present the variations of the magnetic

moment of a particle when  $R = 10000$  with an energy  $E = 600 \text{ keV}$ , that corresponds to an energy close to the one of the separatrix and a motion in the chaotic layer. As seen in Fig. 6, the motion of this particle is chaotic and we notice in Fig. 9 that the variations of  $\bar{\mu}$  are bigger than in the first case, we actually have  $\Delta\bar{\mu}/\bar{\mu} \simeq 20\%$ . In the third case, (lower plot in Fig. 9), we are considering the situation of the particle is moving in a system with the aspect ratios of real tokamaks, namely  $R = 3$  at an energy of  $E = 600 \text{ keV}$ . As anticipated by the left plot in Fig. 8, the particle trajectory is chaotic and the variations of  $\bar{\mu}$  are important  $\Delta\bar{\mu}/\bar{\mu} \simeq 60\%$  and unpredictable. This seems to confirm that in the phase space of such systems, there is no global third constant of the motion. The existence of a constant related to the magnetic moment may be locally true, so we expect the general picture of a mixed phase space with regions of chaos and regions with regular motion. This nevertheless poses the problem of a global reduction performed in for instance gyrokinetics theory in the Maxwell-Vlasov context.

## V. CONCLUSION AND POSSIBLE CONSEQUENCES

Looking for chaos of charged particles trajectories evolving under the influence of a magnetic field with a toroidal structure, as for instance an axi-symmetric one is not an easy issue. One of the main difficulties is to visualize trajectories correctly, and the second problem is to explore the phase space. Given these difficulties, in this paper we choose to highlight the presence of chaos of particle trajectory in two specific cases. First, we take into account a ripple effect, and as such we break a symmetry and the associated exact invariant of the motion. This allows to insure an a priori non-integrable system and to localize and visualize chaos more easily. This step allowed us to insist on the fact that the chaotic motion of charged particles is not directly linked to the chaotic nature of magnetic field lines, as indeed we considered a non generic perturbation which kept the regularity of field lines, while generating chaos in particle trajectories. So this simple example allowed to underline the fact that the link between chaos of particle trajectories and chaos of magnetic field lines is not obvious. In the second case, we considered an axi-symmetric configuration, with two constants of the motion. We managed to observe chaos by tuning the winding profile of magnetic field lines in order to create a separatrix in the effective Hamiltonian of the cylindrical integrable system and perturbing it slowly by adding some curvature and returning back to the toroidal configuration. We exhibited that the chaotic region increases when the aspect ratio (major radius) of the tokamak decreases. At the same time we measured the fluctuations of the magnetic variations of  $\bar{\mu}$  which are also directly correlated with the chaos of the particle trajectories. The presence of chaotic trajectories in the case of an axi-symmetric field implies

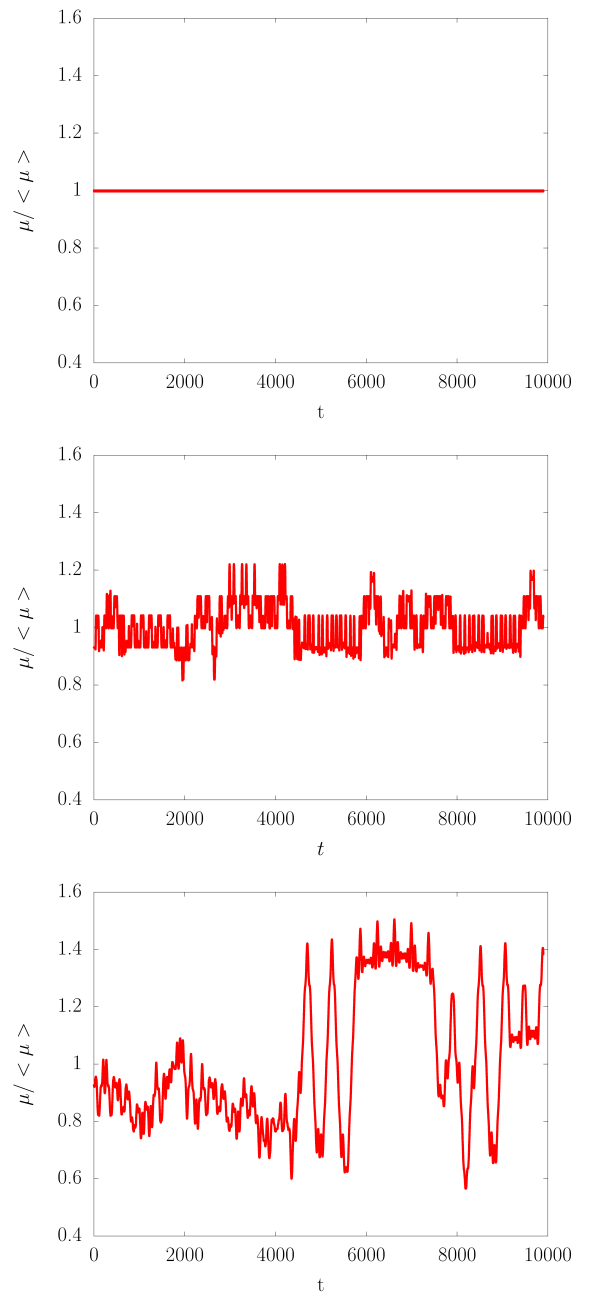


Figure 9: Fluctuation of the finite-time averaged magnetic momentum versus time. The average is performed over about twenty gyration periods. In the upper plot, the values for regular low energy motion versus time are represented,  $R = 10^4$ ,  $E = 450 \text{ keV}$ . We can expect that a third constant of the motion exists. For the middle plot we see fluctuations of about  $\Delta\bar{\mu}/\bar{\mu} \simeq 20\%$ , we still have  $R = 10^4$  but higher energy  $E = 600 \text{ keV}$ . In the lower plot we have fluctuations about 60%, we are in the case of realistic ratios,  $R = 3$  and  $E = 600 \text{ keV}$ . In this last case, it is difficult to imagine that a modified expression of the magnetic moment  $\mu$  would become constant.

that no third constant of the motion exists as the motion is non-integrable. This implies therefore that the magnetic moment can not be a global constant over all phase space, and that this system corresponds likely to a system with mixed phase space, with regions of regular motion and regions of chaotic motion. We may therefore expect all the zoology and complex transport properties that is present in one and a half degrees of freedom system, such as stickiness and associated memory effects. Another consequence is that one has to be careful when performing gyrokinetic reduction. Indeed usually the support of the particle density function described by the Vlasov-Maxwell system covers the whole phase space. Since there are regions with chaos an non-constant magnetic moment, a straightforward reduction is a priori not possible. A future line of research in this field, could be on how to perform the reduction only in specific regions of phase space, and how what remains in the other regions is affecting the dynamics of the reduced distribution. In real case scenarii, it is also likely that regions where the reduction a priori works may be changing with the magnetic and electric fields, leading to possible intermittent reductions, a more thorough study in localizing all these regions in phase space in realistic tokamak like configurations appears therefore as a necessity.

## ANNEXE

In these annexes we used Newton's law, but Noether theorem and a Lagrangian formalism can be more elegant.

### A. Particle trajectory without plasma

In the simple case in which there is no plasma inside tokamak, we can write the magnetic field as :

$$\mathbf{B} = \frac{B_0 R}{\xi} \hat{\mathbf{e}}_\varphi. \quad (23)$$

We apply Newton second law to a charged particle of mass  $m$ , charge  $q$ , moving in this magnetic field. In polar coordinates  $(r, \theta, z)$ , we have :

$$\ddot{r} - r\dot{\theta}^2 = -\frac{B_0 R q}{m r} \dot{z}, \quad (24)$$

$$r\ddot{\theta} + 2\dot{r}\dot{\theta} = 0, \quad (25)$$

$$\ddot{z} = \frac{B_0 R q}{m r} \dot{r}, \quad (26)$$

where if we refer to Fig. 1, we actually have used the notations  $r = \xi$  and  $\theta = \varphi$ . We integrate Eq. (25) and (26) and obtain :

$$r^2 \dot{\theta} = C, \quad (27)$$

$$\dot{z} = \frac{B_0 R q}{m} \ln(r) + C', \quad (28)$$

where  $C$  and  $C'$  are two constants.

We can then use expression (27) and (28) in Eq. (24), multiply it by  $\dot{r}$  and integrate to obtain the effective Hamiltonian

$$\frac{\dot{r}^2}{2} + \frac{C^2}{2r^2} + \frac{(\frac{B_0 R q}{m} \ln(r))^2}{2} + \frac{B_0 R q}{m} C' \ln(r) = H_{eff0}, \quad (29)$$

We end up with an effective Hamiltonian (29) with one degree of freedom, and this shows that particle trajectory in this simple magnetic field is integrable.

### B. Particle trajectory in cylindrical geometry

A very similar calculation can be made in the case of a cylindrical geometry. We recall that the magnetic field is given by

$$\mathbf{B} = B_0 \hat{\mathbf{e}}_z + f(r) \hat{\mathbf{e}}_\theta. \quad (30)$$

We apply Newton second law to a charged particle of mass  $m$ , charge  $q$ , moving in this magnetic field. In polar coordinates  $(r, \theta, z)$ , we obtain:

$$\ddot{r} - r\dot{\theta}^2 = \frac{q}{m} (B_0 r \dot{\theta} - f(r) \dot{z}), \quad (31)$$

$$r\ddot{\theta} + 2\dot{r}\dot{\theta} = -\frac{q B_0}{m} \dot{r}, \quad (32)$$

$$\ddot{z} = \frac{q}{m} \dot{r} f(r), \quad (33)$$

Note that the  $z$ -direction corresponds to axes along the constant  $\hat{\mathbf{e}}_\varphi$  ( $R = \infty$ ), and not the  $z$  depicted in Fig. 1. We integrate Eq. (33), and (32) as well multiplying it by  $r$  before hand and obtain:

$$r^2 \dot{\theta} + \frac{q B_0}{2m} r^2 = A, \quad (34)$$

$$\dot{z} = \frac{q}{m} F(r), \quad (35)$$

where  $A$  is a constant and  $F(r) = \int^r f(x) dx$ .

Now, using expressions (34) and (35) in Eq. (31), which we multiply by  $\dot{r}$  before integration, we end up with:

$$m \frac{\dot{r}^2}{2} + \frac{m A^2}{2r^2} + \frac{(q B_0)^2}{8m} r^2 + \frac{q^2}{m} F^2(r) = H_{eff}, \quad (36)$$

in which  $H_{eff}$  is a constant. This system is also integrable, but contrary to the Hamiltonian (29) presents the interest to allow us to create a separatrix by tuning the function  $F(r)$ , in other words the so called  $q$ -profile.

### Acknowledgments

We are very grateful to P. J. Morrison for providing useful comments and remarks. This work was carried out within the framework the European Fusion Development Agreement and the French Research Federation for Fu-

sion Studies. It is supported by the European Communities under the contract of Association between Euratom and CEA. The views and opinions expressed herein do not necessarily reflect those of the European Commission.

- 
- [1] N. N. Bogoliubov and Y. A. Mitropolsky, *Asymptotic Methods in the Theory of Non Linear Oscillations* (Gordon and Breach, 1961).
  - [2] M. Kruskal, *J. Math. Phys.* **3**, 806 (1962).
  - [3] J. R. Cary and A. J. Brizard, *Rev. mod. Phys.* **81**, 693 (2009).
  - [4] D. d.-C.-N. del Castillo-Negrete and J. J. Martinell, *Communications in Nonlinear Science and Numerical Simulation* **17**, 2031 (2012).
  - [5] F. Porcelli, L.-G. Eriksson, and I. Furno, *Phys. Lett. A* **216**, 289 (1996).
  - [6] L.-G. Eriksson and F. Porcelli, *Plasma Phys. Control. Fusion* **43** (2001).
  - [7] J. Egedal, *Nucl. Fusion* **40**, 1597 (2000).
  - [8] A. I. Neishtadt, *Sov. Phys. Plasma Phys.* **12**, 568 (1986).
  - [9] A. I. Neishtadt, *Celestial Mech. and Dynamical Astronomy* **65**, 1 (1997).
  - [10] D. Benisti and L. Gremillet, *Phys. Plasmas* **14**, 042304 (2007).
  - [11] X. Leoncini, A. Neishtadt, and A. Vasiliev, *Phys. Rev. E* **79**, 026213 (2009).
  - [12] A. I. Neishtadt, A. A. Vasiliev, and A. V. Artemyev, *Regular and Chaotic Dynamics* **18**, 686 (2013).
  - [13] V. Arnold, V. Kozlov, and A. Neishtadt, *Encyclopedia of Mathematical Sciences*, Vol. 3 (Springer-Verlag, 1988).
  - [14] G. Dif-Pradalier, J. Gunn, G. Ciraolo, C. Chang, G. Chiavassa, P. Diamond, N. Fedorczak, P. Ghendrih, L. Isoardi, M. Kocan, S. Ku, E. Serre, and P. Tamain, *J. Nucl. Mater.* (2011).
  - [15] C. S. Gardner, *Phys. Rev.* **115**, 791 (1959).
  - [16] A. Boozer, *Phys. Fluids* **23**, 904 (1980).
  - [17] J. R. Cary and J. D. Hanson, *Phys. Fluids* **29**, 2464 (1986).
  - [18] R. G. Littlejohn, *J. Math. Phys.* **24**, 1730 (1981).
  - [19] X. Leoncini, O. Agullo, M. Muraglia, and C. Chandre, *Eur. Phys. J. B* **53**, 351 (2006).
  - [20] R. I. McLachlan and P. Atela, *Nonlinearity* **5**, 541 (1992).
  - [21] P. N. Yushmanov, *Reviews of plasma physics* **16**, 117 (1990).
  - [22] P. J. Morrison, *Phys. Plasmas* **7**, 2279 (2000).
  - [23] M.-C. Firpo, W. Ettoumi, R. Farengo, H. E. Ferrari, P. L. G. Matinez, and A. F. Lifschitz, *Phys. Plasmas* **20** (2013).
  - [24] T. Evans, A. Wingen, J. Watkins, and K. Spatschek, *Nonlinear Dynamics* ed T. Evans (Rijeka: InTech) (2010).
  - [25] A. Babiano, G. Boffetta, and A. Provenzale, *Phys. Fluids* **6**, 2465 (1994).
  - [26] R. Basu, T. Jessen, V. Naulin, and J. J. Rasmussen, *Phys. Plasmas* **10**, 2696 (2003).
  - [27] S. Benkadda, P. Gabbai, and G. M. Zaslavsky, *Phys. Plasmas* **4**, 2864 (1997).
  - [28] P. Beyer and S. Benkadda, *Chaos* **11**, 774 (2001).
  - [29] B. A. Carreras, V. E. Lynch, L. Garcia, M. Edelman, and G. M. Zaslavsky, *Chaos* **13**, 1175 (2003).
  - [30] G. Ciraolo, F. Briolle, C. Chandre, E. Floriani, R. Lima, M. Vittot, M. Pettini, C. Figarella, and P. Ghendrih, *Phys. Rev. E* **69** (2004).
  - [31] J. S. E. Portela, I. L. Caldas, R. L. Viana, and P. Morrison, *Int. J. Bifurcation Chaos* **17** (2007).